

See discussions, stats, and author profiles for this publication at: <https://www.researchgate.net/publication/12204741>

Direct FeS Cluster Involvement in Generation of a Radical in Lysine 2,3-Aminomutase †

ARTICLE *in* BIOCHEMISTRY · JANUARY 2001

Impact Factor: 3.02 · DOI: 10.1021/bi0022184 · Source: PubMed

CITATIONS

77

READS

20

5 AUTHORS, INCLUDING:



Perry Allen Frey

University of Wisconsin–Madison

282 PUBLICATIONS **9,559** CITATIONS

SEE PROFILE



Robert A Scott

University of Georgia

192 PUBLICATIONS **6,250** CITATIONS

SEE PROFILE

Direct FeS Cluster Involvement in Generation of a Radical in Lysine 2,3-Aminomutase[†]

Nathaniel J. Cospér,[‡] Squire J. Booker,[§] Frank Ruzicka,^{||} Perry A. Frey,^{||} and Robert A. Scott^{*,‡}

Department of Chemistry, University of Georgia, Athens, Georgia 30602-2556, Department of Biochemistry and Molecular Biology, Pennsylvania State University, University Park, Pennsylvania 16802, and Department of Biochemistry, University of Wisconsin, Madison, Wisconsin 53705

Received September 20, 2000; Revised Manuscript Received October 30, 2000

ABSTRACT: Lysine 2,3-aminomutase (KAM) belongs to a class of enzymes that use FeS clusters and *S*-adenosyl-L-methionine to initiate radical-dependent chemistry. Selenium K-edge X-ray absorption spectroscopic analysis of KAM poised at various stages of catalysis, in the presence of selenomethionine or Se-adenosyl-L-selenomethionine, reveals that the cofactor is cleaved only in the presence of dithionite and the substrate analogue *trans*-4,5-dehydrolysine. A new Fourier transform peak at 2.7 Å, assigned as a Se–Fe interaction, appears concomitant with this cleavage. This is the first demonstration of a direct interaction of *S*-adenosyl-L-methionine, or its cleavage products, with the FeS cluster in this class of enzymes.

In recent years, mechanistic details of a new class of *S*-adenosyl-L-methionine (AdoMet)¹-dependent enzymes have begun to emerge (1, 2). These enzymes use Fe₄S₄ clusters in combination with AdoMet to generate enzyme-bound, carbon-centered radicals, which are obligatory intermediates in the corresponding reactions. The importance of this radical-generating system is underscored by the diversity of reactions and the difficult chemistry in which it participates. Many of these reactions are anaerobic counterparts to those that are typically catalyzed by copper- or iron-dependent monooxygenases and dioxygenases. Although others are presumed to exist, four enzymes within this class have been characterized in moderate detail. They include biotin synthase (3, 9, 10), pyruvate formate lyase activating enzyme (PFL-activase) (4, 5), anaerobic ribonucleotide reductase activating enzyme (ARR-activase) (6), and lysine 2,3-aminomutase (KAM) (7, 8). Very recent studies suggest that these and other biosynthetic and metabolic enzymes form a superfamily of radical-generating AdoMet-dependent enzymes (H. J. Sofia, personal communication). Other potential members

of this superfamily are also involved in vitamin (thiamin) and cofactor (heme, bacteriochlorophyll, molybdopterin, and nitrogenase) biosynthesis.

Biotin synthase, the apparent product of the *bioB* gene, catalyzes the final step, insertion of sulfur into dethiobiotin, in the biosynthesis of this essential vitamin. Two unactivated hydrogens from the precursor are removed in the process, and 2 mol of AdoMet is expended per mole of biotin that is synthesized (9, 10). PFL-activase and ARR-activase catalyze the formation of a stable radical that is situated on the backbone of a glycine residue of the respective cognate proteins, pyruvate formate lyase (PFL) and anaerobic ribonucleoside triphosphate reductase (ARR) (11–13). PFL catalyzes the reversible condensation of acetyl-CoA and formate, producing pyruvate and CoA (14), while ARR catalyzes the production of deoxyribonucleoside triphosphates from the corresponding ribonucleoside triphosphate precursors (15). Both of these enzymes are central to the anaerobic metabolism of *Escherichia coli* and are present in other obligate or facultative anaerobes. In each case, the glycy radical acts as an initiator of chemistry that is postulated to proceed by radical-dependent mechanisms (14, 15). One mole of AdoMet is expended per mole of glycy radical that is generated; however, the glycy radical is regenerated after each turnover and, therefore, serves as a cofactor (6, 16, 17). KAM, isolated from *Clostridium subterminale* SB4, catalyzes the interconversion of L- α -lysine and L- β -lysine (Scheme 1). This is the initial step in the catabolism of the amino acid to acetyl-CoA and ammonia, which are usable carbon and nitrogen sources for the bacterium (18, 19). Thus, the enzymes in this class catalyze a range of chemical conversions that are essential to biosynthetic and metabolic pathways in numerous organisms.

The KAM holoenzyme is composed of six identical subunits (*M_r* = 47 kDa) and contains one pyridoxal 5'-phosphate (PLP) and one Zn per subunit, in addition to the

[†] This research was supported by the National Institutes of Health (Grant GM 42025 to RAS), startup funds from Pennsylvania State University (to SJB), and the National Institute of Diabetes and Digestive and Kidney Diseases (Grant DK 28607 to PAF). NJC has been supported by a National Science Foundation Research Training Group (NSF RTG) award to the Center of Metalloenzyme Studies (DR 90-14281) and is currently being supported by a NSF RTG in Prokaryotic Diversity traineeship (BIR-9143235).

^{*} To whom correspondence should be addressed. E-mail: rscott@uga.edu.

[‡] University of Georgia.

[§] Pennsylvania State University.

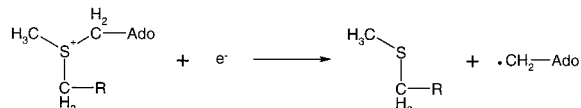
^{||} University of Wisconsin.

¹ Abbreviations: AdoMet, *S*-adenosyl-L-methionine; AdoSeMet, Se-adenosyl-L-selenomethionine; ARR, anaerobic ribonucleotide reductase; EPR, electron paramagnetic resonance; EXAFS, extended X-ray absorption fine structure; FeS, iron–sulfur cluster; FT, Fourier transform; KAM, lysine 2,3-aminomutase; Met, methionine; PFL, pyruvate formate lyase; SeMet, selenomethionine; XAS, X-ray absorption spectroscopy.

Scheme 1: Conversion of L- α -Lysine to L- β -Lysine, Catalyzed by Lysine 2,3-Aminomutase



Scheme 2: Generation of Methionine and the 5'-Deoxyadenosyl Radical by Cleavage of a Sulfur–Carbon Bond in AdoMet^a



^a Replacement of the sulfur with selenium supports KAM catalysis and provides a “spectroscopic handle”.

iron and sulfide that constitute the Fe₄S₄ center (8, 19–21). The reaction it catalyzes is functionally equivalent to those that have been historically considered to lie exclusively within the domain of coenzyme B₁₂-containing enzymes; however, the enzyme neither contains this cofactor nor is activated by it (22). Instead, stoichiometric amounts of AdoMet are sufficient to render it maximally active in the presence of a suitable reductant (dithionite or deazaflavin and light) (7, 23).

Numerous mechanistic studies have led to a model in which the 5'-deoxyadenosyl moiety of AdoMet acts as an intermediate carrier of hydrogen during the reaction (22, 24, 25). This is realized via the reductive cleavage of the cofactor to methionine and 5'-deoxyadenosine 5'-yl, which initiates catalysis in the forward direction by abstracting the 3-*proR* hydrogen of α -lysine (24). After rearranging to the product radical via a PLP-stabilized azocyclopropylcarbinyl radical, the product radical reabstracts a hydrogen atom from 5'-deoxyadenosine to complete the reaction, and reafford 5'-deoxyadenosine 5'-yl (3, 26).

The cleavage of AdoMet to 5'-deoxyadenosine 5'-yl is an unprecedented biochemical reaction. The stoichiometry of the reaction requires input of an electron, which is provided by the reduced iron–sulfur cluster ([Fe₄S₄]⁺) (6, 7). Several mechanisms to account for the cleavage of AdoMet can be envisioned (1, 3). In the simplest case, the iron–sulfur cluster transfers an electron into the sulfonium of AdoMet, causing it to be fragmented into methionine and 5'-deoxyadenosine 5'-yl (Scheme 2). Alternatively, AdoMet might serve to adenosylate a bridging sulfide of the cluster. Homolytic cleavage of the sulfur–carbon bond would then yield a 5'-deoxyadenosyl radical, and an oxidized FeS cluster. Other proposals invoke participation of an iron atom of the cluster. For instance, a 5'-deoxyadenosyl radical could derive from homolytic cleavage of an Fe–carbon bond.

To obtain insight into the mechanism of AdoMet cleavage in KAM, we used selenium K-edge X-ray absorption spectroscopy (XAS) in combination with the selenium derivative of AdoMet, Se-adenosyl-L-selenomethionine (AdoSeMet), to follow the course of the cleavage reaction. AdoSeMet is a known substrate for many AdoMet-dependent methylases and AdoMet decarboxylases, and in some cases supports faster turnover than the normal substrate (27–30). The rate of turnover of KAM with the AdoSeMet is more than half of that with AdoMet, verifying that this is an appropriate analogue with which to study the cleavage reaction (23).

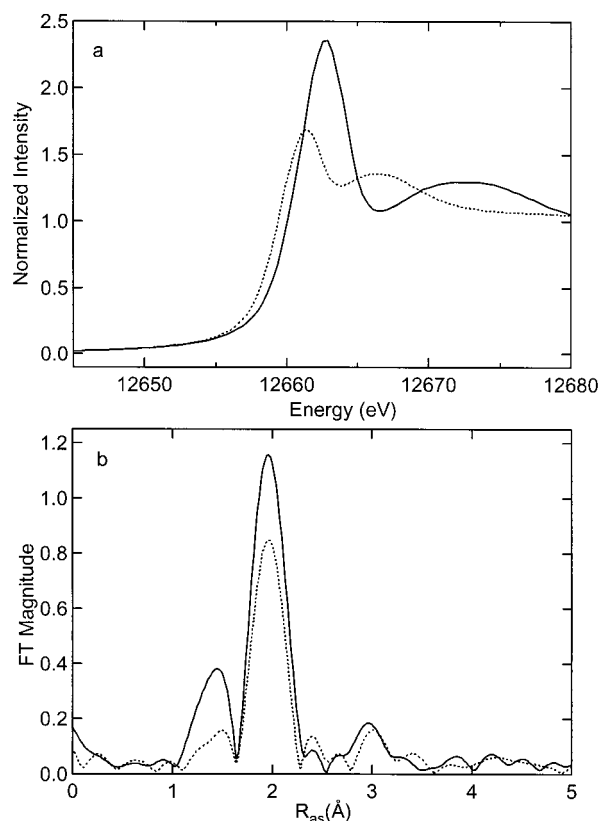


FIGURE 1: Se K-edge X-ray absorption spectra (a) and Fourier transforms (b; over $k = 2\text{--}12.5 \text{ \AA}^{-1}$) of Se-adenosyl-L-selenomethionine (AdoSeMet, solid line) and L-selenomethionine (SeMet; dotted line).

MATERIALS AND METHODS

XAS data were collected at Stanford Synchrotron Radiation Laboratory (SSRL), beamline 7-3, with the SPEAR storage ring operating in a dedicated mode at 3.0 GeV and 60–100 mA. Fluorescence data were collected using a Ge solid state array detector and a Si(220) double-crystal monochromator that was 50% detuned. Calibration was achieved using an elemental Se standard (first inflection, 12 658 eV). EXAFS analysis was performed with the EXAFSPAK software (www-ssrl.slac.stanford.edu/exafspak.html), according to standard procedures (31). Fourier transform plots were generated with sulfur-based phase correction. Both Se and Zn XAS data were collected on the same samples, and in most cases, duplicate preparations of similar samples were analyzed.

Typical EXAFS samples contained 200 mM sodium EPPS buffer (pH 8.0), 536 μM KAM (holoenzyme, three FeS clusters per hexamer), 1.6 mM AdoSeMet or SeMet, and 3.4 mM *trans*-4,5-dehydrolysine or L-lysine. When included, 5'-deoxyadenosine was at a concentration of 3.6 mM, and the concentration of sodium dithionite was 2.6 mM. The enzyme was reductively incubated in the absence of iron, desalted by gel filtration, concentrated, and added to a mixture of the other components of the reaction. After 10 min at ambient temperature, the reaction mixture was mixed with an equal volume of anaerobic 50% glycerol, loaded into an XAS cuvet, and frozen in liquid N₂. The concentration of all components of the reaction mixture was therefore diluted by a factor of 2. All steps involving preparation of

Table 1: Curve Fitting Results for EXAFS of Se Models^a

sample, file name (<i>k</i> range), $\Delta k^3\chi$	fit	shell	N_s	R_{as} (Å)	σ_{as}^2 (Å ²)	ΔE_0 (eV)	f'^b
Se-methionine, EMETA (2–12.5 Å ⁻¹), $\Delta k^3\chi = 5.34$	1	Se–C	1	1.94	–0.0017	–0.03	0.100
	2	Se–C	2	1.93	0.0015	–3.44	0.088
	3	Se–C	3	1.92	0.0041	–7.29	0.116
	5	Se–C	2	1.93	0.0015	–4.64	0.086
		Se–C	1	2.89	0.0052		
Se-methionine, EMETB (2–12.5 Å ⁻¹), $\Delta k^3\chi = 5.45$	6	Se–C	2	1.93	0.0012	–4.00	0.091
	7	Se–C	2	1.93	0.0012	–4.00	0.087
		Se–C	1	2.84	0.0043		
Se-adenosyl-L-selenomethionine (SeSAM), ESAMA (2–12.5 Å ⁻¹), $\Delta k^3\chi = 6.45$	8	Se–C	2	1.94	0.0003	0.28	0.095
	9	Se–C	3	1.93	0.0025	–1.97	0.097
	10	Se–C	4	1.92	0.0044	–4.95	0.122
	11	Se–C	3	1.92	0.0024	–3.69	0.093
		Se–C	1	2.85	0.0021		
Se-adenosyl-L-selenomethionine (SeSAM), ESAMB (2–12.5 Å ⁻¹), $\Delta k^3\chi = 6.32$	12	Se–C	3	1.94	0.0020	–0.73	0.097
	13	Se–C	3	1.94	0.0020	–0.85	0.091
		Se–C	1	2.86	0.0011		

^a Group is the chemical unit defined for the multiple-scattering calculation. N_s is the number of scatterers (or groups) per metal. R_{as} is the metal–scatterer distance. σ_{as}^2 is the mean-square deviation in R_{as} . ΔE_0 is the shift in E_0 , which is the energy at which the EXAFS begin, for the theoretical scattering functions. $\Delta k^3\chi$ is the amplitude of the EXAFS oscillations, which is used to normalize the goodness of fit values. ^b f' is a normalized error (χ^2): $f' = (\{\sum_i [k^3(\chi_i^{obs} - \chi_i^{calc})]^2 / N\}^{1/2}) / [(k^3\chi^{obs})_{max} - (k^3\chi^{obs})_{min}]$.

XAS samples, including freezing, were carried out inside of a Coy anaerobic chamber.

The use of *trans*-4,5-dehydrolysine, in lieu of the normal substrate, was essential to generating a sufficient quantity of the intermediate state for successful XAS analysis. Upon abstraction of the 3-*proR* hydrogen by 5'-deoxyadenosine 5'-yl, a stable allylic radical is formed, which does not have sufficient energy to partition backward by reabstraction of a hydrogen atom from 5'-deoxyadenosine. The result is that near-stoichiometric amounts of the products of AdoMet cleavage are generated (32). In contrast, with the normal substrate, less than 10% of this intermediate accumulates if the reaction mixture is frozen in the steady state. Substantially smaller amounts accumulate as the reaction approaches equilibrium.

RESULTS

XAS spectra were acquired for selenomethionine (SeMet) and AdoSeMet, and then compared with spectra of these molecules bound to KAM under different conditions, and poised at various stages in the catalytic cycle. Se K-edge XAS investigation of SeMet and AdoSeMet reveals the expected change in edge position and a significant change in edge shape (Figure 1), making Se edges a diagnostic fingerprint for distinguishing between samples that resemble these two compounds. The shift in absorption edge position between SeMet (12 659.6 eV inflection) and AdoSeMet (12 661.2 eV) is indicative of a change in the Se oxidation state of the sample (33).

Concomitant with this edge change is a reduction in Fourier transform (FT) peak intensity, which is indicative of the coordination number for SeMet being lower than that for AdoSeMet. First-shell EXAFS for SeMet are fit best assuming two carbon atoms at 1.93 Å (fits 2 and 6 in Table 1), while first-shell EXAFS for AdoSeMet are fit best assuming three carbons at 1.94 Å (fits 9 and 12 in Table 1). In the Fourier transforms of both SeMet and AdoSeMet, there is a small peak at ca. 3 Å (Figure 1b). The EXAFS contribution to this peak can be fit, with reasonable Debye–

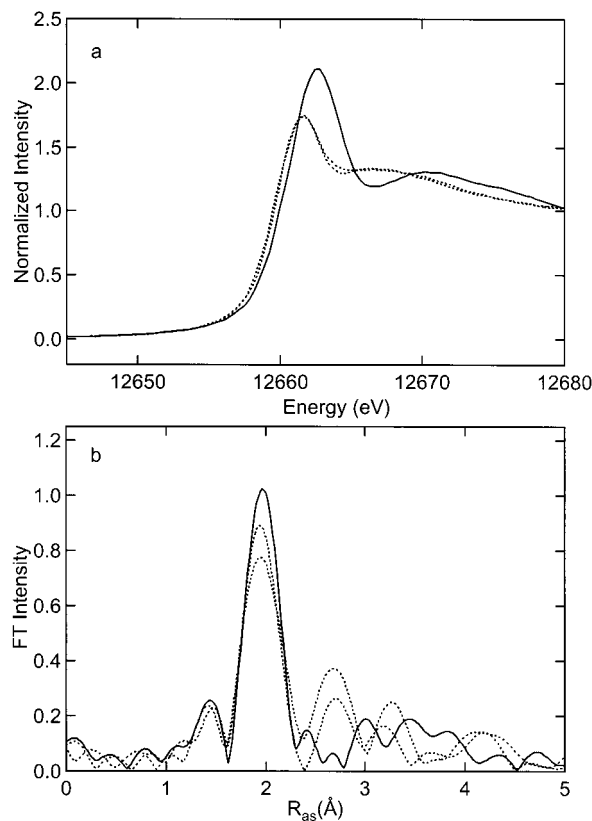


FIGURE 2: Se K-edge X-ray absorption spectra (a) and Fourier transforms (b; over $k = 2$ –12.5 Å⁻¹) of KAM incubated with AdoSeMet and dithionite (solid line) or AdoSeMet, dithionite, and *trans*-3,4-dehydrolysine (dotted line, duplicate samples).

Waller factor values, assuming a carbon scatterer at 2.8–2.9 Å (fits 5, 7, 11, and 13 in Table 1).²

Incubating KAM with stoichiometric amounts of AdoSeMet with (Figure 2, solid) or without dithionite yields Se-edge and FT spectra that are similar to that of AdoSeMet alone (Figure 1, solid). The EXAFS for this sample are best fit assuming three carbon scatterers at 1.93 Å (fits 2 and 6 in

Table 2: Curve Fitting Results for Se EXAFS of KAM Incubated with Se Compounds^a

sample, file name (<i>k</i> range), $\Delta k^3\chi$	fit	shell	N_s	R_{as} (Å)	σ_{as}^2 (Å ²)	ΔE_0 (eV)	f'
KAM and AdoSeMet, ELOEA (2–12.5 Å ⁻¹), $\Delta k^3\chi = 8.03$	1	Se–C	2	1.94	0.0000	0.56	0.104
	2	Se–C	3	1.93	0.0021	–1.33	0.101
	3	Se–C	4	1.92	0.0039	–3.96	0.115
	4	Se–C	3	1.93	0.0021	–3.15	0.098
	5	Se–Fe Se–C	1 3	2.88 1.93	0.0168 0.0021	–2.01	0.100
KAM and AdoSeMet, ELOEB (2–12.5 Å ⁻¹), $\Delta k^3\chi = 10.00$	6	Se–C	3	1.93	0.0012	–2.22	0.092
	7	Se–C	3	1.94	0.0013	–1.65	0.089
		Se–C	1	2.92	0.0029		
KAM, AdoSeMet, dithionite, and dehydrolysine, ELAEA (2–12.5 Å ⁻¹), $\Delta k^3\chi = 8.21$	8	Se–C	1	1.93	–0.0022	–1.65	0.101
	9	Se–C	2	1.93	0.0010	–4.48	0.092
	10	Se–C	3	1.92	0.0033	–7.53	0.102
	11	Se–C	2	1.93	0.0010	–5.18	0.086
		Se–Fe	1	2.65	0.0121		
	12	Se–C	2	1.92	0.0010	–5.63	0.093
		Se–C	1	2.97	0.0002		
	13	Se–C	2	1.92	0.0006	–4.89	0.082
KAM, AdoSeMet, dithionite, and dehydrolysine, ELAEB (2–12.5 Å ⁻¹), $\Delta k^3\chi = 8.16$		Se–Fe	1	2.67	0.0113		
		Se–C	1	2.94	–0.0007		
	14	Se–C	2	1.93	0.0019	–5.40	0.119
	15	Se–C	3	1.92	0.0044	–7.36	0.126
	16	Se–C	2	1.93	0.0020	–4.18	0.099
KAM, SeMet, and 5'-deoxyadenosine, ELSEA (2–12.5 Å ⁻¹), $\Delta k^3\chi = 6.33$		Se–Fe	1	2.67	0.0088		
		Se–C	1	2.95	–0.0017		
	17	Se–C	1	1.96	–0.0009	2.20	0.135
	18	Se–C	2	1.95	0.0025	0.49	0.127
	19	Se–C	3	1.93	0.0054	–5.31	0.142
	20	Se–C	2	1.94	0.0025	–2.59	0.126
		Se–Fe	1	2.86	0.0166		
KAM, SeMet, 5'-deoxyadenosine, and dehydrolysine, ELQEA (2–12.5 Å ⁻¹), $\Delta k^3\chi = 8.75$	21	Se–C	2	1.94	0.0025	–1.69	0.124
		Se–C	1	2.88	0.0009		
	22	Se–C	1	1.92	–0.0020	–5.07	0.132
	23	Se–C	2	1.92	0.0011	–6.48	0.127
	24	Se–C	3	1.92	0.0035	–8.58	0.133
	25	Se–C	2	1.93	0.0010	–4.58	0.101
		Se–Fe	1	2.64	0.0059		
	26	Se–C	2	1.91	0.0014	–9.23	0.121
		Se–C	1	2.95	–0.0035		
	27	Se–C	2	1.93	0.0011	–4.62	0.098
		Se–Fe	1	2.64	0.0065		
		Se–C	1	2.94	–0.0005		

^a See the footnotes of Table 1.

Table 2). As with SeMet and AdoSeMet, this spectrum exhibits a peak at ca. 3 Å, which can be fit assuming a single carbon scatterer at 2.88 Å (fits 5 and 7 in Table 2).

In contrast, incubating KAM with AdoSeMet, dithionite, and the substrate analogue, *trans*-4,5-dehydrolysine, yields a Se-edge spectrum that is reminiscent of SeMet (Figure 2, dotted lines). This indicates that AdoSeMet has been cleaved to form SeMet and 5'-deoxyadenosine. Importantly, the Se environment in this sample differs from free SeMet by the presence of a new, reproducible peak at ca. 2.7 Å in the FT (Figure 2b, dotted lines). The EXAFS for KAM incubated with AdoSeMet, dithionite, and *trans*-4,5-dehydrolysine are best fit assuming two carbon scatterers at 1.93 Å (fits 9 and 14 in Table 2). The new ca. 2.7-Å FT peak can be successfully modeled as a first-row transition metal. Since Zn K-edge XAS shows that the divalent cation site in KAM does not change at any stage of catalysis (Supporting Information), this peak is interpreted as a selenium–iron interaction with an interatomic distance of 2.67 Å (fits 11, 13, and 16 in Table 2). XAS “sees” an average coordination

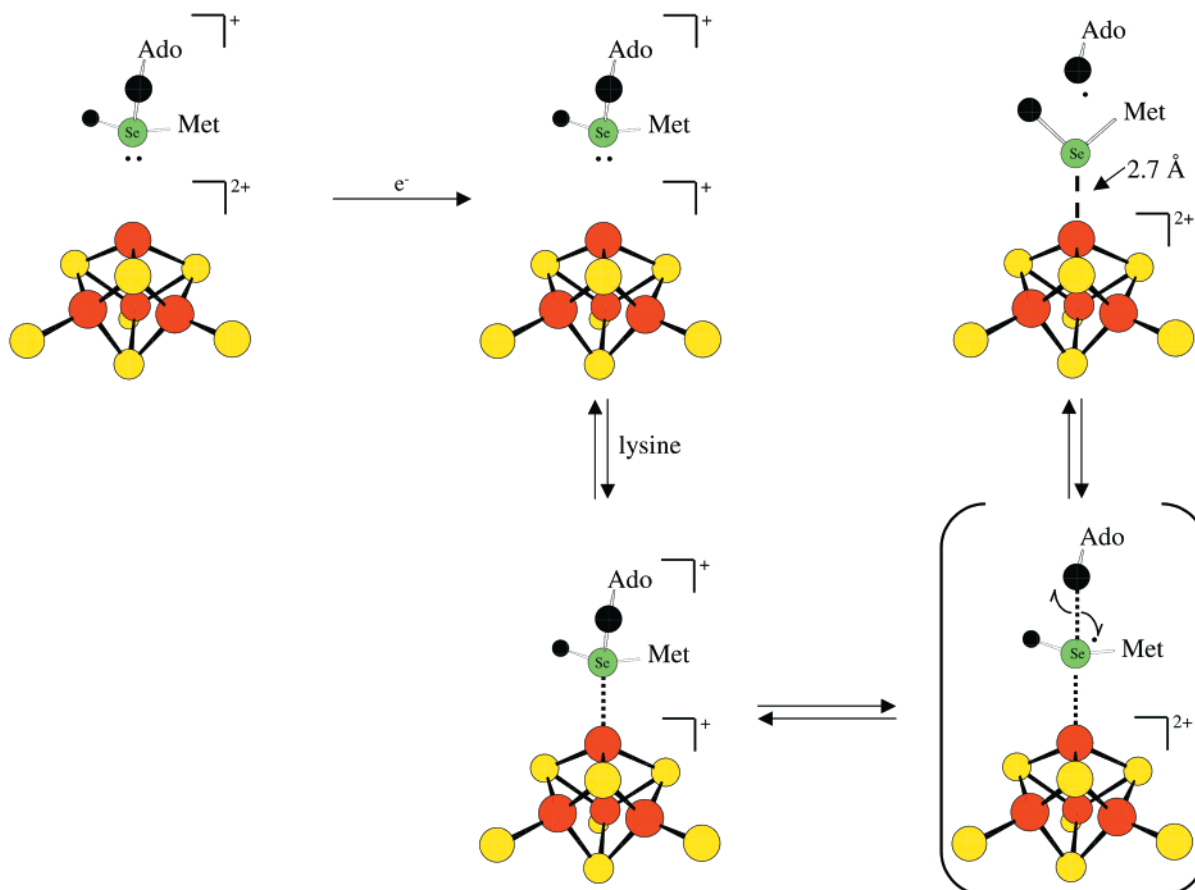
environment for all molecules of a given element in the sample. Thus, Fe XAS would see an average of the four Fe atoms in the Fe₄S₄ cluster and would not be sensitive to the addition of a Se atom at only one Fe.

This intermediate cannot be generated simply by adding SeMet and 5'-deoxyadenosine to the [Fe₄S₄]²⁺ state of KAM (Figure 3, solid line); however, it is formed if *trans*-4,5-dehydrolysine (Figure 3, dotted line) or lysine is included (data not shown). The EXAFS for KAM incubated with SeMet and 5'-deoxyadenosine are best fit assuming two carbon atoms at 1.95 Å (fit 18 in Table 2). The EXAFS for KAM incubated with SeMet, 5'-deoxyadenosine, and *trans*-4,5-dehydrolysine are best fit assuming two carbon scatterers at 1.93 Å and a first-row transition metal at 2.64 Å, which simulates the EXAFS contribution for the new 2.7 Å peak (fits 25 and 27 in Table 2). As with KAM samples incubated with AdoSeMet, dithionite, and *trans*-4,5-dehydrolysine, this metal is interpreted as an iron atom. This behavior is completely consistent with a true intermediate state rather than adventitious binding, especially since no more than stoichiometric amounts of selenomethionine were used.

DISCUSSION

The need for lysine or *trans*-4,5-dehydrolysine to effect cleavage of AdoMet and to observe the subsequent interac-

² Although inclusion of the 2.9 Å Se–C scatterer does not significantly improve the goodness of fit value, f' , this shell is needed as a baseline parameter for subsequent fits.

Scheme 3: Proposed Mechanism for Generation of the 5'-Deoxyadenosyl Radical in Lysine 2,3-Aminomutase^a

^a This scheme is shown with an empty coordination site for the top Fe in the cube. Although this coordination site is most likely filled during some stages of catalysis, our XAS data do not provide any evidence for the identity or occupancy of this putative ligand.

tion is consistent with recent results with *S*-3',4'-anhydroadenosyl-L-methionine (3',4'-anAdoMet). This AdoMet analogue supports turnover, albeit at a highly reduced rate. More importantly, it allows observation of the surrogate 5'-deoxyadenosyl radical via its allylic stabilization. However, no cleavage of the cofactor is observed unless the substrate or substrate analogue is present (34). This suggests a mechanism for cleavage in which substrate binding induces a conformational change that brings the nonbonding electron pair of the sulfonium in proximity to one of the irons of the FeS cluster. This might raise the redox potential of AdoMet to that which would allow inner-sphere electron transfer from the FeS cluster, with concerted cleavage of the carbon–sulfur bond.

The appearance of a FT peak at 2.7 Å, which is explained as a selenium–iron interaction, concomitant with the change in edge position and reduction in the intensity of the main FT peak, indicates that AdoSeMet is cleaved to SeMet, which associates with the FeS cluster. This suggests that the mechanism for generation of the 5'-deoxyadenosyl radical in KAM involves iron-based chemistry (Scheme 3) and renders an intermediate involving an iron–carbon bond unlikely. The interaction of selenomethionine with the iron–sulfur cluster suggests a unique Fe site in the Fe₄S₄ cluster. This is consistent with previous electron paramagnetic resonance (EPR) spectroscopic studies on KAM, in which nearly stoichiometric amounts of [Fe₃S₄]¹ clusters were

generated when the enzyme was treated with oxygen or ferricyanide (8). This behavior is reminiscent of aconitase, which is known to cycle between Fe₃S₄ and Fe₄S₄ clusters, with loss of the iron that has a water or hydroxide ligand in place of a protein-derived cysteine ligand.

KAM is distinct within this class of AdoMet-dependent enzymes in that the cleavage of the cofactor is freely reversible. We postulate that the interaction of methionine with the FeS cluster might aid not only in cleaving the cofactor, but also in maintaining the methionine in place for the back reaction, and influencing the energetics of this process.

ACKNOWLEDGMENT

We thank Profs. Michael K. Johnson and Cheves Walling for insightful discussions and for critical comments regarding the manuscript. The XAS data were collected at SSRL, which is operated by the Department of Energy, Division of Chemical Sciences. The SSRL Biotechnology program is supported by the National Institutes of Health, Biomedical Resource Technology Program, Division of Research Resources.

SUPPORTING INFORMATION AVAILABLE

Curve-fitting results and Zn XAS data. This material is available free of charge via the Internet at <http://pubs.acs.org>.

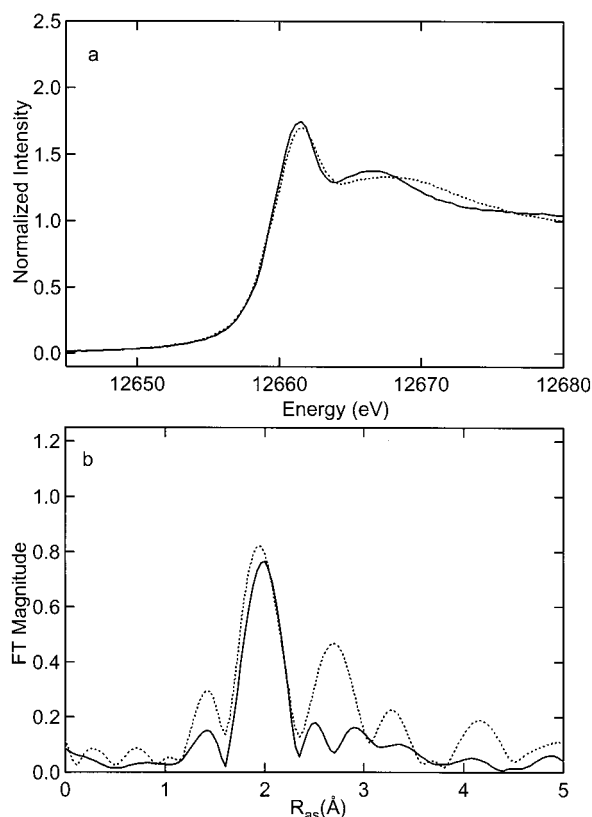


FIGURE 3: Se K-edge X-ray absorption spectra (a) and Fourier transforms (b; over $k = 2\text{--}12.5 \text{ \AA}^{-1}$) of KAM incubated with SeMet and 5'-deoxyadenosine (solid line) or SeMet, 5'-deoxyadenosine, and *trans*-3,4-dehydrolysine (dotted line).

REFERENCES

1. Frey, P. A., and Booker, S. J. (1999) in *Advances in Free Radical Chemistry* (Zard, S. Z., Ed.) Vol. 2, JAI Press Inc., Stamford, CT.
2. Johnson, M. K. (1998) *Curr. Opin. Chem. Biol.* 2, 173–181.
3. Frey, P. A., and Reed, G. H. (1992) *Adv. Enzymol. Relat. Areas Mol. Biol.* 66, 1–39.
4. Külzer, R., Pils, T., Kappl, R., Hüttermann, J., and Knappe, J. (1998) *J. Biol. Chem.* 273, 4897–4903.
5. Broderick, J. B., Duderstadt, R. E., Fernandez, D. C., Wojtuszewski, K., Henshaw, T. F., and Johnson, M. K. (1997) *J. Am. Chem. Soc.* 119, 7396–7397.
6. Ollagnier, S., Mulliez, E., Schmidt, P. P., Eliasson, R., Gaillard, J., Deronzier, C., Bergman, T., Graslund, A., Reichard, P., and Fontecave, M. (1997) *J. Biol. Chem.* 272, 24216–24223.

7. Lieder, K. W., Booker, S., Ruzicka, F. J., Beinert, H., Reed, G. H., and Frey, P. A. (1998) *Biochemistry* 37, 2578–2585.
8. Petrovich, R. M., Ruzicka, F. J., Reed, G. H., and Frey, P. A. (1992) *Biochemistry* 31, 10774–10781.
9. Shaw, N. M., et al. (1998) *Biochem. J.* 330, 1079–1085.
10. Guianvarc'h, D., Florentin, D., Bui, B. T. S., Nunzi, F., and Marquet, A. (1997) *Biochem. Biophys. Res. Commun.* 236, 402–406.
11. Knappe, J., Neugebauer, F. A., Blaschkowski, H. P., and Gänzler, M. (1984) *Proc. Natl. Acad. Sci. U.S.A.* 81, 1332–1335.
12. Sun, X., et al. (1996) *J. Biol. Chem.* 271, 6827–6831.
13. Wagner, A. F. V., Frey, M., Neugebauer, F. A., Schäfer, W., and Knappe, J. (1992) *Proc. Natl. Acad. Sci. U.S.A.* 89, 996–1000.
14. Kessler, D., and Knappe, J. (1996) in *Escherichia Coli and Salmonella, Cellular and Molecular Biology* (Neidhart, F. C., Ed.) American Society for Microbiology, Washington, DC.
15. Reichard, P. (1993) *J. Biol. Chem.* 268, 8383–8386.
16. Stubbe, J., and Donk, W. A. v. d. (1998) *Chem. Rev.* 98, 705–762.
17. Knappe, J., Elbert, S., Frey, M., and Wagner, A. F. V. (1993) *Biochem. Soc. Trans.* 21, 731–734.
18. Chirpich, R. P., Zappia, V., Costilow, R. N., and Barker, H. A. (1970) *J. Biol. Chem.* 245, 1178–1189.
19. Costilow, R. N., Rochovansky, O. M., and Barker, H. A. (1966) *J. Biol. Chem.* 241, 1573–1580.
20. Song, K. B., and Frey, P. A. (1991) *J. Biol. Chem.* 266, 7651–7655.
21. Ruzicka, F. J., Lieder, K. W., and Frey, P. A. (2000) *J. Bacteriol.* 182, 469–476.
22. Frey, P. A. (1993) *FASEB J.* 7, 662–670.
23. Booker, S. J., unpublished results.
24. Aberhart, D. J., Gould, S. J., Lin, H.-J., Thiruvengadam, T. K., and Weiller, B. H. (1983) *J. Am. Chem. Soc.* 105, 5461–5470.
25. Moss, M. L., and Frey, P. A. (1990) *J. Biol. Chem.* 265, 18112–18115.
26. Ballinger, M. D., and Reed, G. H. (1992) *Biochemistry* 31, 945–949.
27. Bremer, J., and Natori, Y. (1960) *Biochim. Biophys. Acta* 44, 367–370.
28. Mudd, S. H., and Cantoni, G. L. (1957) *Nature* 180, 1052.
29. Pegg, A. E. (1969) *Biochim. Biophys. Acta* 177, 361–364.
30. Wu, M., and Wachsmann, J. T. (1971) *J. Bacteriol.* 105, 1222–1223.
31. Scott, R. A. (1985) *Methods Enzymol.* 117, 414–459.
32. Wu, W., Booker, S., Lieder, K. W., Bandarian, V., Reed, G. H., and Frey, P. A. (2000) *Biochemistry* 39, 9561–9570.
33. Pickering, I. J., George, G. N., Fleet-Stalder, V. V., Chasteen, T. G., and Prince, R. C. (1999) *J. Biol. Inorg. Chem.* 4, 791–794.
34. Magnusson, O. T., Reed, G. H., and Frey, P. A. (1999) *J. Am. Chem. Soc.* 121, 9764–9765.

BI0022184